

Electron density and implication for bonding in CuB. Jiang,^{1,*} J. Friis,² R. Holmestad,² J. M. Zuo,³ M. O’Keeffe,⁴ and J. C. H. Spence¹¹*Department of Physics and Astronomy, Arizona State University, Tempe, Arizona 85287, USA*²*Department of Physics, Norwegian University of Science and Technology (NTNU), 7491 Trondheim, Norway*³*Department of Material Science and Engineering, University of Illinois, Urbana, Illinois 61801, USA*⁴*Department of Chemistry, Arizona State University, Tempe, Arizona 85287, USA*

(Received 7 October 2003; revised manuscript received 29 March 2004; published 23 June 2004)

We report highly accurate measurements for the low-order Fourier components of the crystal potential in copper. These were obtained by transmission electron diffraction using a small probe and multiple scattering analysis. They were used to refine the Cu 3*d* radial wave function. An accurate charge-deformation map and a 3*d* orbital radial wave function were obtained by using a multipole refinement of the structure factors obtained from combined quantitative electron diffraction and γ -ray diffraction measurements. The results show a large change in the 3*d* orbital radial function from *d*-band formation and *d*-*s* band crossing (*d*-*s* hybridization). Band theory calculations are in excellent agreement with the measurements and show that the charge deformation in Ag is very similar to that in Cu. Our findings are in general agreement with the monovalent description of these metals.

DOI: 10.1103/PhysRevB.69.245110

PACS number(s): 71.20.Be, 32.80.Cy, 95.30.Ky, 71.15.Mb

I. INTRODUCTION

The measurement of valence electron radial wave functions and charge densities has long been recognized as a challenging problem. It requires highly accurate Fourier components of charge density and a sound multipole refinement model. The Fourier components of charge density are equal to the x-ray structure factors, whose amplitude, in principle, can be obtained experimentally by measuring the diffraction intensities. In simple inorganic materials like copper, it is difficult to obtain the crucial low-order structure factors by kinematic photon (x-ray or γ -ray) diffraction with sufficient accuracy for charge density analysis due to uncertainties in extinction corrections and other factors.¹ Recently, γ -ray diffraction at energies up to 400 kV has been used with radiation whose wavelength is about the same (0.03 Å) as that used for electron diffraction. Primary extinction is reduced when the extinction distance (which increases with beam energy) exceeds the mosaic block size. Secondary extinction is also reduced, but not eliminated. The extinction correction method proposed by Palmer *et al.*² using multiwavelength extinction-affected Bragg intensities is used, based on the two beam dynamical diffraction model of Zacharisen *et al.*³ This extrapolates Bragg intensities to zero wavelength, and claims to provide an extinction-free measurement, which has been applied to several crystals.^{2,4,5} Its accuracy has been questioned by Streltsov *et al.*,⁵ who has applied this method on Al₂O₃. For strong low order reflections, they conclude for Al₂O₃ that “extrapolation is generally not unique, and extended extrapolation of multiwavelength Bragg intensities to the zero-interaction limit is only of limited accuracy.”⁵ Electron diffraction, on the other hand, is inherently more sensitive for small scattering vectors, and is free from extinction effects, so that low order structure factors can be obtained with much higher accuracy.¹ The

consistency of the quantitative convergent-beam electron diffraction technique (QCBED) method has been tested for rutile.^{6,7} This work showed that QCBED is a robust method for accurate low order structure factor measurement. Using a combination of electron (for low order) and x-ray (for higher order) diffraction data, detailed information about the valence electron distributions has recently been obtained in several simple inorganic crystals.^{5,7-11}

Here we present our recent results for Cu and Ag, using experimental electron diffraction, band theory calculations, and multipole analysis. We find that a large change in the *d*-orbital radial wave function is required in the multipole model to account for the differences in x-ray structure factors of crystals, and that obtained by superimposing spherical atoms. Brewer’s hypothesis,¹² that the binding energy per electron is approximately constant for metals, is also discussed.

II. METHOD

In the multipole model, the atomic charge density in a crystal is expanded into three parts; the spherical inner-shell electrons (core electrons), spherical valence shells (monopoles), and a series of nucleus-centered local symmetry-adapted spherical harmonic functions which reflect the small but important nonspherical valence charge distribution (higher order multipoles). The x-ray structure factors are fitted by adjusting the refinement parameters (monopoles and multipoles). Following Hansen and Coppens,¹³ the charge of a pseudoatom is described as

$$\rho_{\text{pseudoatom}}(\vec{r}) = P_c * \rho_{\text{core}}(r) + P_v * \kappa^3 * \rho_{\text{valence}}(\kappa r) + \sum_{l=1}^{l_{\text{max}}} R_l(\alpha_l r) \sum_{m=0}^l P_{lm} d_{lm\pm}(\theta, \phi). \quad (1)$$

The first and second terms represent the spherical atomic core, which is well described by atomic modeling and is

TABLE I. Measured (QCBED) and calculated structure factors for Cu. The column headed $3d^{10}4s$ is a multipole refinement with fixed orbital occupation and using neutral atom orbitals for $3d$ and $4s$; the column headed $3d_{\text{crystal}}^{10}4s$ is a multipole refinement with $3d_{\text{crystal}}$ orbital ($3d_{\text{crystal}}=3d^{10-n}4s^n$ with $3d$ orbital wave function from Cu^{2+} and $4s$ from neutral atom, and gives the best refined value of $n=1.27$). The residual R calculated for the seven structure factors listed shows the agreement of theory with QCBED experiment. The experimental structure factors are converted to their 0 K static values. The unit of x-ray structure factors is electrons per cell.

hkl or R	$s=\sin(\theta)/\lambda$	QCBED	DFT theory (GGA)	Neutral atom model	$3d^{10}4s$ multipole refinement	$3d_{\text{crystal}}^{10}4s$ multipole refinement
111	0.240	86.76(16)	86.80	88.18	87.94	86.81
200	0.278	81.76(16)	81.52	82.71	82.47	81.67
220	0.393	66.72(12)	66.70	66.99	66.74	66.75
311	0.460	58.94(08)	59.02	59.00	58.77	58.99
222	0.481	56.96(32)	56.89	56.80	56.58	56.84
400	0.555	49.80(40)	49.93	49.68	49.49	49.82
440	0.785	35.41(16)	35.44	35.27	35.17	35.40
$R(\%)$			0.15	0.71	0.64	0.08

fixed in our multipole refinement, and the spherical (monopole) valence charge density, respectively. The third term is a summation over the multipoles. It should be noted that the first two terms are real charge densities, while the third term only redistributes valence density nonspherically in real space. The volume integration of this term is zero. Slater type orbitals (STO) calculated by multiconfiguration Dirac–Fock (MCDHF)¹⁴ were used for the density functions of the core, $\rho_{\text{core}}(r)$, and valence electron monopole, $\rho_{\text{valence}}(\kappa r)$. The valence shell can be further divided into two monopoles to simulate charge transfer between different orbitals on the same atom site (orbital hybridization effect) or the orbital deformation effect. The multipole radial functions, $R_l(\kappa r)$, are calculated using single exponential functions, or an atomic orbital product. This simple model can produce meaningful information on bonding, as demonstrated in several cases, such as TiO_2 , MgO , Cu_2O , and Si .^{7,10,11,15} In the copper refinement, the radial function of the hexadecapole is constructed from a $3d^*3d$ orbital wave function self-product. In this case, the radial scaling factor κ is refined. For copper, there is only one cubic harmonics left. Thus, Eq. (1) can be written for copper as

$$\begin{aligned} \rho_{\text{pseudoatom}}(\vec{r}) = & P_c * \rho_{\text{core}}(r) + P_{3d} * \kappa_{3d}^3 * \rho_{3d}(\kappa_{3d}r) \\ & + P_{4s} * \kappa_{4s}^3 * \rho_{4s}(\kappa_{4s}r) \\ & + P_{\text{hex}} * \kappa_{3d}^3 * \rho_{3d}(\kappa_{3d}r) * K_{41}, \end{aligned} \quad (2)$$

where K_{41} is a fourth-order cubic harmonic. The refinement parameters are the valence electron radial function scaling factor, κ_{3d} and κ_{4s} , and the multipole populations, P_{hex} . In Sec. III, we discuss this formula again to show that the second term needs further modification to fit experimental measurement.

Accurate measurements of the low-order structure factors were made using the QCBED method that we have developed recently.¹⁶ The experiment was performed using a LEO-912 in-column Ω -energy-filtering transmission electron

microscope (TEM) with a Gatan liquid nitrogen cooled sample holder. The TEM specimen used is a Cu foil sample prepared by electrolytic polishing and cooled down to 105 K to reduce phonon scattering. The electron beam-heating effect was considered and refined to be about 5 K.⁸ A 10 eV energy-filtering slit was placed around the zero-loss peak to remove the contribution from inelastically scattered electrons, which form a background due to plasmon and other loss processes. Off-zone-axis systematic diffraction patterns were collected for seven low order reflections and recorded on a Gatan CCD camera. The “EXTAL” software package¹⁶ was used for CBED refinement—this takes full account of multiple scattering and “absorption” in the Bloch-wave formalism. The small electron probe size (about 10 nm diameter) ensures that the data are collected within a single mosaic block.

Band theory calculations were performed using the augmented plane wave plus local orbital method (APW+lo),¹⁷ as implemented in the program WIEN2K.¹⁸ Exchange and correlation effects are treated within density functional theory, using the generalized gradient approximation (GGA).¹⁹ We used fully relativistic calculations for core electrons, and scalar relativistic for valence electrons. The muffin tin (MT) radius was 2.0 a.u. The Brillouin-zone integration was performed using a modified tetrahedron method.²⁰ The k -point convergence was tested using a total of 10 000 k points in the unit cell with $R_{\text{mt}} * K_{\text{max}}$ equal to 7.0. Basis size is 71 (with 12 local orbitals) for Cu and 78 (with 13 local orbitals) for Ag. Spin-orbit (SO) coupling was also tested for Ag, but it was found that the resulting changes in structure factors were less than 0.01% for low order reflections. Hence we consider the spin-orbit effect unimportant in Ag, and it is not considered.

III. RESULTS AND DISCUSSION

We have measured the seven lowest-order inequivalent structure factors for copper using QCBED. These are reported in Table I. Also reported in the table are the results of band theory calculation and multipole models. It is seen that

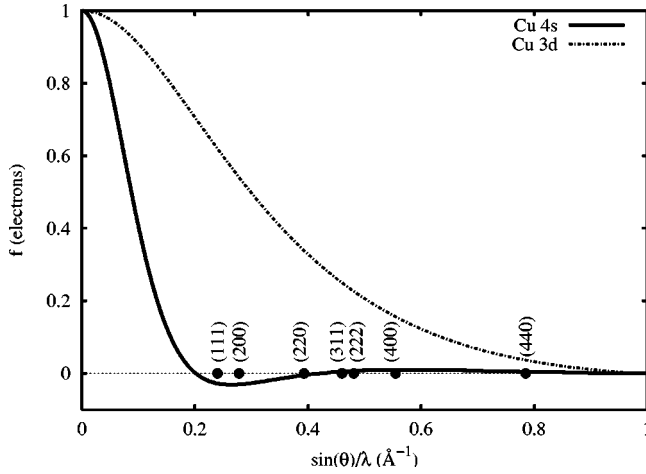


FIG. 1. Scattering factors of Cu 3d and 4s orbitals. The scattering angles of the lowest order reflections are shown. Note that the contribution to these reflections from the 4s orbital is small.

theory and experiment are in excellent agreement. This is an important observation as the experimental results come with (small) error bars and they thus serve to provide limits on the possible errors of the theory.

The QCBED data were merged with γ -ray diffraction measurements^{21,22} for the higher orders (where electron diffraction is less accurate than x ray), and the combination subject to multipole refinement using the program VALRAY.²³ To combine the two data sets, the first seven measured electron structure factors were transformed to their corresponding static x-ray structure factors at 0 K, and then used to replace the γ -ray diffraction values reported by Petrillo *et al.*²¹ The refinement parameters are the electron populations in the valence shell orbitals (monopoles), one cubic hexadecapole, with corresponding radial scaling parameters. It is seen from Table I that there are significant differences between the multipole fits and QCBED/theory for low orders. To understand the origin of these differences, the scattering factors of Cu orbitals are plotted in Fig. 1.

We see that the 4s orbital affects reflections below $s = 0.2 \text{ \AA}^{-1}$ ($s = \sin \theta / \lambda$ is the scattering vector), and contributes to small negative values between $s = 0.2$ and $s = 0.4$, while the 3d orbital contributes at higher scattering angles up to $s = 0.8$. This analysis suggests that the differences in the x-ray structure factors for (111) ($s = 0.24 \text{ \AA}^{-1}$), (200), (220), and (311) cannot be attributed to changes in the 4s orbital. A large deformation in the 3d orbital radial wave function must be responsible for these differences. To find a suitable model for multipole refinement, we see that for the low order reflections, the measured x-ray structure factors are systematically lower than those for neutral atoms, indicating partial delocalization of the 3d orbital electrons. We suggest that the 3d orbital radial wave function has a tail that does not contribute significantly to the measured reflections. We simulate this effect by using a $3d_{\text{crystal}}$ orbital function constructed from 3d orbitals of neutral or ionic atom plus a delocalized tail. Thus, the 3d radial wave function in copper is written in two parts, with one localized and one diffuse, such as

TABLE II. Multipole refinement results for Cu and Ag. Refinements use the ion core, plus a d orbital from a d^9 configuration (d orbital in Cu^{+2} or Ag^{+2} ion) and 4s or 5s orbitals from neutral atoms. Multipoles up to fourth order are chosen for refinement. The allowed multipoles are selected according to the index-picking rules of Kurki-Suonio (Ref. 30). The d -orbital deformation is included in the refinement (by refining n). The 4s or 5s electron population (P_s) is fixed at one. The corresponding kappa for monopoles or multipoles is refined. [Note, Dawson normalization is used for multipole populations, see VALRAY manual for details (Ref. 23).]

Parameters	Cu	Ag
n	1.27(6)	1.35(1)
κ_d	1.006(5)	1.0083(7)
κ_s	1.1(1)	1.15(1)
P_{hex}	-0.0004(7)	0.08(2)
R	0.06%	0.02%

$\rho(3d_{\text{crystal}}) = \rho(3d^{10-n}) + \rho(3d_{\text{diffused}}^n)$ (n is a refinement parameter), using small changes in the radial scaling factors to simulate the 3d radial wave-function deformation effects in the crystal. When compared with the 3d orbital in a neutral atom, $\rho(3d_{\text{diffused}})$ is a much more diffuse function than the $\rho(3d)$ orbital wave function in a Cu neutral atom. This function must satisfy two conditions: to keep the total crystal charge neutral, and to spread the 3d orbital electrons out to a larger distance from the nucleus. For simplicity, we can use a kappa-modified 4s orbital of the Cu neutral atom for $3d_{\text{diffused}}$. By writing $3d_{\text{crystal}}$ in this form [$\rho(3d_{\text{crystal}}) = \rho(3d^{10-n}) + \rho(4s^n)$], we treat the 4s orbital in the crystal and the delocalized part of $3d_{\text{crystal}}$ together, using a single kappa parameter. This is a convenient way of doing multipole refinement and eliminates one kappa parameter in the refinement. Note especially, however, that the number n measures the degree of 3d orbital electron spreading in real space, but has no physical meaning regarding 3d to 4s orbital promotion. Thus, Eq. (2) can be further modified by considering 3d orbital deformation as follows:

$$\begin{aligned} \rho_{\text{pseudoatom}}(\vec{r}) = & P_c * \rho_{\text{core}}(r) + (10 - n) * \kappa_{3d}^3 * \rho_{3d}(\kappa_{3d}r) \\ & + n * \kappa_{4s}^3 * \rho_{4s}(\kappa_{4s}r) + P_{4s} * \kappa_{4s}^3 * \rho_{4s}(\kappa_{4s}r) \\ & + P_{\text{hex}} * \kappa_{3d}^3 * \rho_{3d}(\kappa_{3d}r) * K_{41}, \end{aligned} \quad (3)$$

where the second and third terms represent the deformed 3d orbital, and the third and fourth terms can be combined together in the refinement. There are four refinement parameters, the numbers n , k_{4s} , k_{3d} , and P_{hex} , as shown in Table II. k_{3d} and n are related to the 3d orbital, and so they affect low order reflections up to $s = 0.8$. There are more than 10 reflections up to $s = 0.8$, therefore k_{3d} and n are overdetermined and refined very accurately. On the other hand, k_{4s} and P_{hex} affect very few low order reflections, and produce results with a much larger percentage error. P_{hex} is smaller from multipole refinement, almost zero. We also evaluated a multipole

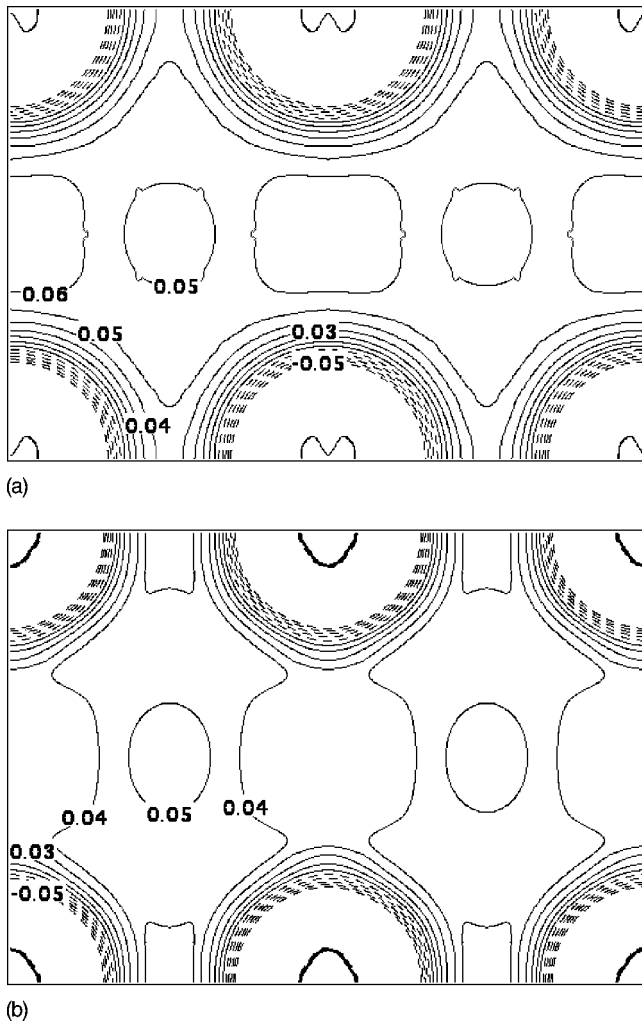


FIG. 2. Valence charge-density deformation map on the (110) plane of copper. The map shows the difference between an experimental valence charge density or theoretical valence charge density and a promolecule valence model as reference. (The promolecule is an artificial crystal made up of superimposed neutral atoms.) The dashed lines are contours with $\Delta\rho < 0$, the solid lines are contours with $\Delta\rho > 0$; the increment between contours is $0.01 e/\text{\AA}^3$. (a) QCBED measurement [valence charge density–neutral atom model of Su *et al.* (Ref. 14)]. (b) Band theory calculation (GGA) [valence charge density (GGA calculation)–neutral atom model (GGA calculation)]. Note, features on both maps are quite similar. There is about $0.05 e/\text{\AA}^3$ charge efficiency in the interstitial regions.

refinement without the P_{hex} term. The change in residual was very small. Thus the, P_{hex} term is not important, and can be omitted in our multipole refinement.

This has proved to be a good approximation, as shown by the multipole refinement results given in Table I. The results are given for a neutral-atom ($3d^{10}4s$) model (only radial scale parameters are refined); for a $3d_{\text{crystal}}^{10}4s$ model (where refinement includes $3d$ orbital deformation), and an agreement index R factor (residual), calculated from the seven QCBED measurements alone. It is found that a $3d_{\text{crystal}}$ function constructed from the d orbital of the d^9 electron configuration ($3d$ orbital in Cu^{+2} ion) produces a better fit in

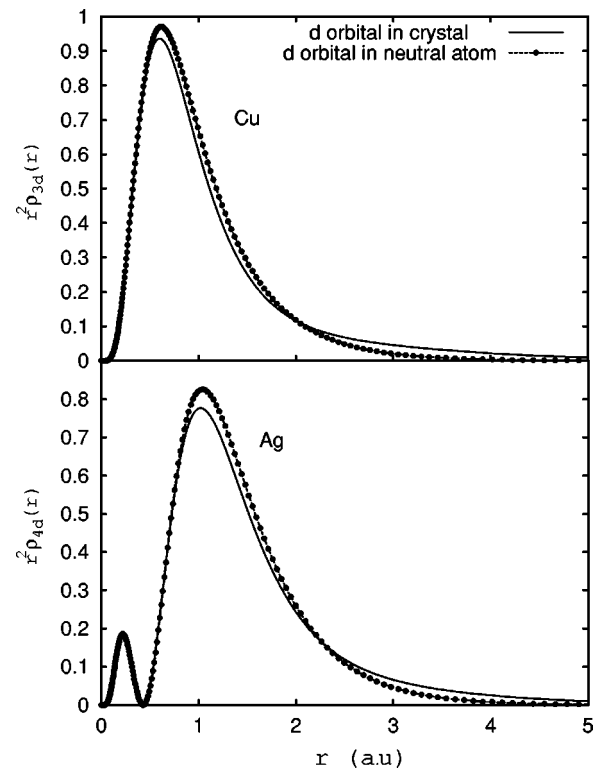


FIG. 3. Cu $3d$ and Ag $4d$ orbital radial probability distribution plots. The valence d orbitals in the crystal spread outward, owing to d -band formation and d - s band hybridization. This kind of deformation cannot be simulated by refining scaling parameters in the multipole model. This charge density is obtained using the second and third terms in Eq. (3). The charge density peak of the $4s$ or $5s$ orbitals at the nucleus ($r=0$) is omitted to construct $3d_{\text{crystal}}$ or $4d_{\text{crystal}}$ orbitals which conform to the requirement that the d orbital approach zero at $r=0$. This has a negligible effect on scattering factors.

the multipole refinement, indicating that the localized $3d$ orbitals are more like $3d$ orbitals in Cu^{+2} ions, due to the reduced screening effect of delocalized $3d$ electrons. For the $3d^{10}4s$ model, $R=0.64\%$ and the fit is outside the range of experimental error [note especially (111) and (200)]. For the $3d_{\text{crystal}}^{10}4s$ model, $R=0.08\%$ (8 times less) and all calculated values agree with experiment within experimental error. The refined value of n is 1.27(6) (Table II).

The resulting valence charge density difference map shown in Fig. 2 shows a spherical charge deficiency region (0.9\AA in radius) around the copper atom and a charge surplus region between atoms. The charge surplus in the interstitial region is about $0.05 e/\text{\AA}^3$, or a 25% increase in valence electron density, which shows a similar feature to band theory calculations. Note the small hexadecapole population, which indicates a very small nonspherical charge deformation (see Table II). Charge redistribution due to this is less than $10^{-6} e/\text{\AA}^3$ between nearest-neighbor atoms, much smaller than the valence electron density, which is about $0.2 e/\text{\AA}^3$. Thus, the covalent contribution to bonding can be neglected. This finding agrees with the theoretical results of Ogata *et al.*,²⁴ who concluded that Cu has a homogeneous charge distribution with little bond directionality.

TABLE III. Slater orbital parameters of Cu $3d$ and Ag $4d$ radial wave functions. The radial wave function $R_{nl}(r)$ is defined by $R_{nl}(r) = \sum_i c_i \chi_i(r)$, where $\chi_i(r) = (2n_i!)^{-1/2} (2z_i)^{n_i+1/2} r^{n_i-1} e^{-z_i r}$. See Clementi *et al.* (Ref. 31) for details.

Crystal	Parameters	Values							
Cu	n	3	3	3	3	3			
	c	0.029 47	0.158 22	0.529 16	0.335 76	0.236 00			
	z	1.800 63	9.011 60	4.811 77	2.377 01	0.913 09			
Ag	n	3	3	3	3	4	4	4	4
	c	0.006 32	0.096 93	0.308 63	-0.457 37	0.071 10	-0.558 14	-0.307 14	-0.105 01
	z	34.018 46	15.420 14	7.718 13	5.101 49	13.671 76	3.493 71	1.707 72	0.800 52

There are two possible interpretations of the refined number n . Brewer¹² has proposed that the electronic configuration in copper is $3d^{10-n}4s^14p^n$, with $n=1.5$. This hypothesis, with $3d$ electrons being promoted into $4p$ free-electron-like orbitals, is used to explain the strong cohesion in noble metals, such as Cu, Ag, Au, but has been questioned by several researchers.²⁵ This first possible explanation of our refinement would assume dsp hybridization, with 1.27 electrons promoted from the $3d$ to the $4sp$ orbital. However, owing to the e_g and t_{2g} energy splitting (about 1 eV) in that case, the charge deformation density would be nonspherical, there would be intense white lines in L_3 -edge electron energy-loss spectra (EELS) and x-ray absorption spectra (XAS), and the $3d$ orbital holes would be expected to give rise to magnetic properties similar to those of the lighter $3d$ metals. However experimental results show that EELS and XAS spectra have no white lines,²⁶ copper is a weakly diamagnetic metal,²⁵ and our charge density refinement shows a spherical deformation density. The ratio of the e_g and t_{2g} orbital electron populations is $1.999\ 94(14)/3$ calculated from the multipole population,⁸ equal to $4/6$ within error. Thus, the nonspherical charge deformation is negligible, in strong contrast to the highly nonspherical distribution found for the formal d^{10} shell of Cu in Cu_2O .¹⁰ Further evidence in support of a monovalent model in copper comes from the free-electron plasma oscillations. The number of free electrons per atom contributing to the plasmon is $1.04(4)$, $[n = (m^* \varepsilon_0 V_{\text{cell}} / \hbar^2 e^2) E_p^2]$, where m^* is the electron effective mass and E_p is the plasmon energy, as calculated using the free-electron model from the first plasmon energy, using $E_p = 9.3$ eV from measured optical properties and the free-electron mass.²⁷ This is in agreement with a monovalent description of Cu. An additional plasmon peak, however, also occurs at $E_p = 19.3$ eV (not due to double scattering),²⁸ and if we use the free-electron plasmon model we then obtain 3.4 electrons per atom contributing to the bulk plasmon from this second peak. These 3.4 electrons may however stem from the relatively delocalized $3d$ electrons. The two volume plasmon energies in copper thus reflect the different properties of free electrons, and those of delocalized $3d$ electrons.

The second interpretation possible is that the Cu $3d$ orbital has large deformation, and so becomes much more diffuse compared with the neutral-atom ground state $3d$ orbital. Our discussions of the preceding four paragraphs support this interpretation. Multipole refinement quantitatively measures the $3d$ -band orbital radial wave function in Cu, which

is shown in Fig. 3. It is constructed from the $3d^{10-n}4s^n$ electron configuration (with $\kappa_{3d} = 1.006$, $\kappa_{4s} = 1.1$, see Table II). We see that the $3d$ orbital in Cu has a long tail, and electrons are delocalized. Experimental Slater orbital parameters were fitted and are given in Table III. This kind of deformation cannot be simulated by refining radial scaling factors alone in the multipole model. That is the reason for the failure of the ground state neutral-atom model. It has been proposed that $3d$ band electrons contribute substantially to the cohesive energy of Cu by $d-s$ orbital hybridization.²⁹ Thus of the total cohesive energy of 0.26 Ry, the calculated contribution from the $4s$ band is 0.11 Ry and thus $d-s$ orbital hybridization contributes significantly to the cohesive energy of Cu (note that the renormalization energy is -0.04 Ry for Cu, therefore, $d-s$ orbital hybridization contributes 0.19 Ry).²⁹

We have also completed a multipole refinement for silver, to measure the $4d$ orbital deformation. Calculated x-ray structure factors were used and refined using similar refinement procedures. The results are listed in Table II. We conclude that charge deformation is again spherical (from the small multipole population) and the $4d$ orbital in silver has a similar amount of deformation to the $3d$ orbital in copper. The ratio of the e_g to t_{2g} orbital electron populations is $2.013(3)/3$, and again the charge deformation is very close to spherical. The Ag $4d$ orbital radial wave function is shown in Fig. 3 and the Slater orbital parameters are given in Table III. The number of free electrons, from the plasmon energy ($E_p = 9.2$ eV) is 1.0.²⁷ We conclude that Ag is a monovalent metal.

It is important to point out that the orbital radial wave functions are deduced from the charge density refinement based on an atomic model. It is well known however, that electrons form bands in crystals and so lose their individuality. Our refinement thus provides an example of how a one-electron model can nevertheless retain useful validity in the transition metals. We expect that this method can also be used in the transition metal compounds, where valence d orbitals form d bands.

IV. SUMMARY

Accurate low order electron structure factors have been measured for copper by quantitative convergent-beam

electron diffraction. Charge density deformation maps refined using a multipole model show a spherical charge deformation in copper and silver. Valence d orbital radial wave functions obtained from multipole refinement, show a large deformation when compared with neutral atoms. Results support the monovalent metal model in Cu and Ag.

ACKNOWLEDGMENTS

This paper was funded by DOE Contract No. DE-FG03-02ER45596 (J.C.H.S.). J.F. was funded by Research Council of Norway (NFR), project 135270/410. Thanks to Dr. P. Rez (ASU) and Dr. P. Blaha (Vienna Tech.) for helpful discussions.

*Electronic mail: jiangb@asu.edu

- ¹B. Jiang, J. M. Zuo, Q. Chen, and J. C. H. Spence, *Acta Crystallogr., Sect. A: Found. Crystallogr.* **A58**, 4 (2002).
- ²A. Palmer and W. Jauch, *Acta Crystallogr., Sect. A: Found. Crystallogr.* **A51**, 662 (1995).
- ³W. H. Zachariasen, *Acta Crystallogr.* **23**, 558 (1967).
- ⁴T. Lippmann and J. R. Schneider, *J. Appl. Crystallogr.* **33**, 156 (2000); A. Kirfel, H. G. Krane, P. Blaha, K. Schwarz, and T. Lippmann, *Acta Crystallogr., Sect. A: Found. Crystallogr.* **A57**, 663 (2001).
- ⁵V. A. Streltsov, P. N. H. Nakashima, and A. W. S. Johnson, *J. Phys. Chem. Solids* **62**, 2109 (2001).
- ⁶B. Jiang, J. M. Zuo, J. Friis, and J. C. H. Spence, *Microsc. Microanal.* **9**, 457 (2003).
- ⁷B. Jiang, J. M. Zuo, N. Jiang, M. O'Keeffe, and J. C. H. Spence, *Acta Crystallogr., Sect. A: Found. Crystallogr.* **A59**, 341 (2003).
- ⁸J. Friis, B. Jiang, J. C. H. Spence, and R. Holmestad, *Microsc. Microanal.* **9**, 379 (2003).
- ⁹J. Friis, G. H. K. Madsen, F. K. Larsen, B. Jiang, K. Martinsen, and R. Holmestad, *J. Chem. Phys.* **119**, 11 359 (2003); M. A. Tabbarnor, A. F. Fox, and R. M. Fisher, *Acta Crystallogr., Sect. A: Found. Crystallogr.* **A46**, 165 (1990).
- ¹⁰J. M. Zuo, M. Kim, M. O'Keeffe, and J. C. H. Spence, *Nature (London)* **401**, 49 (1999).
- ¹¹J. M. Zuo, M. O'Keeffe, P. Rez, and J. C. H. Spence, *Phys. Rev. Lett.* **78**, 4777 (1997).
- ¹²L. Brewer, in *Structure and Bonding in Crystals*, edited by M. O'Keeffe and A. Navrotsky (Academic, New York, 1982), Vol. I, p. 143; *Science* **161**, 115 (1968).
- ¹³H. K. Hansen and P. Coppens, *Acta Crystallogr., Sect. A: Cryst. Phys., Diffr., Theor. Gen. Crystallogr.* **A34**, 909 (1978).
- ¹⁴Z. W. Su and P. Coppens, *Acta Crystallogr., Sect. A: Found. Crystallogr.* **A54**, 646 (1998); P. Macchi and P. Coppens, *ibid.* **A57**, 656 (2001).
- ¹⁵J. M. Zuo, P. Blaha, and K. Schwarz, *J. Phys.: Condens. Matter* **9**, 7541 (1997).
- ¹⁶J. C. H. Spence and J. M. Zuo, *Electron Microdiffraction* (Plenum, New York, 1992); J. M. Zuo, *Mater. Trans., JIM* **39**, 938 (1998).
- ¹⁷E. Sjøstedt, L. Nordstrom, and D. J. Singh, *Solid State Commun.* **114**, 15 (2000).
- ¹⁸K. Schwarz, P. Blaha, and G. K. H. Madsen, *Comput. Phys. Commun.* **126**, 71 (2002).
- ¹⁹J. P. Perdew, K. Burke, and M. Ernzerhof, *Phys. Rev. Lett.* **77**, 3865 (1996).
- ²⁰P. E. Blochl, O. Jepsen, and O. K. Andersen, *Phys. Rev. B* **49**, 16 223 (1994).
- ²¹C. Petrillo, F. Sacchetti, and G. Mazzone, *Acta Crystallogr., Sect. A: Found. Crystallogr.* **A54**, 468 (1998).
- ²²J. R. Schneider, N. K. Hansen, and H. Kretschmer, *Acta Crystallogr., Sect. A: Cryst. Phys., Diffr., Theor. Gen. Crystallogr.* **A37**, 711 (1981); J. R. Schneider, *ibid.* **A33**, 235 (1977); J. R. Schneider, *J. Appl. Crystallogr.* **9**, 394 (1976).
- ²³R. F. Stewart, M. A. Spackman, and C. Flensburg, *Valray User's Manual* (Carnegie Mellon University and University of Copenhagen, 2000).
- ²⁴S. Ogata, J. Li, and S. Yip, *Science* **298**, 807 (2002).
- ²⁵W. Hume-Rothery, *The Structure of Metals and Alloys* (The Chaucer Press Ltd., London, 1969); P. S. Rudman, J. Stringer, and R. I. Jaffee, *McGraw-Hill Series in Materials Science* (McGraw-Hill, Geneva and Villar, Switzerland, 1966).
- ²⁶C. Bonnelle, *Ann. Phys. (Paris)* **1**, 439 (1966); M. H. Heinonen and J. A. Leiro, *Philos. Mag. B* **49**, L43 (1984); R. D. Leapman, L. A. Grunes, and P. L. Fejes, *Phys. Rev. B* **26**, 614 (1982); S. Kiyono, S. Chiba, Y. Hayasi, S. Kato, and S. Mochimaru, *Jpn. J. Appl. Phys.* **17**, 212 (1978); J. Luitz, M. Maier, C. Hebert, P. Schattschneider, P. Blaha, K. Schwarz, and B. Jouffrey, *Eur. Phys. J. B* **21**, 363 (2001).
- ²⁷H. Ehrenreich and H. R. Philipp, *Phys. Rev.* **128**, 1622 (1962).
- ²⁸J. Deniel, C. Festenberg, H. Reather, and K. Zeppenfeld, *Springer Tracts in Modern Physics* (Springer, New York, 1970), Vol. 54, p. 101.
- ²⁹C. D. Gelatt, H. Ehrenreich, and R. E. Watson, *Phys. Rev. B* **15**, 1613 (1977).
- ³⁰K. Kurki-Suonio, *Isr. J. Chem.* **16**, 115 (1977).
- ³¹E. Clementi and C. Roetti, *At. Data Nucl. Data Tables* **14**, 177 (1974).